HDL-TR-1736

Transient Currents in Partially Shielded Conductors: A Circuit Model

November 1975

THIS RESEARCH WAS SPONSORED BY THE DEFENSE NUCLEAR AGENCY UNDER SUBTASK R99QAXEB075 AND WORK UNIT 43/CURRENT INJECTION TECHNIQUES FOR C^3 APPLICATIONS.

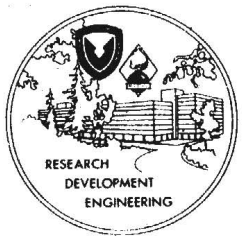

U.S. Army Materiel Command
HARRY DIAMOND LABORATORIES
Adelphi, Maryland 20783

The findings in this report are not to be construed as an official Department of the Army position unless so designated by other authorized documents.

Citation of manufacturers' or trade names does not constitute an official indorsement or approval of the use thereof.

Destroy this report when it is no longer needed. Do not return it to the originator.

UNCLASSIFIED

SECURITY CLASSIFICATION OF THIS PAGE *(When Data Entered)*

REPORT DOCUMENTATION PAGE		READ INSTRUCTIONS BEFORE COMPLETING FORM
1. REPORT NUMBER HDL-TR-1736	2. GOVT ACCESSION NO.	3. RECIPIENT'S CATALOG NUMBER
4. TITLE *(and Subtitle)* Transient Currents in Partially Shielded Conductors: A Circuit Model		5. TYPE OF REPORT & PERIOD COVERED Technical Report 6. PERFORMING ORG. REPORT NUMBER
7. AUTHOR(s) Richard L. Monroe		8. CONTRACT OR GRANT NUMBER(s) NWER Subtask: R99QAXEBO75
9. PERFORMING ORGANIZATION NAME AND ADDRESS Harry Diamond Laboratories 2800 Powder Mill Road Adelphi, MD 20783		10. PROGRAM ELEMENT, PROJECT, TASK AREA & WORK UNIT NUMBERS Work Unit: 43 Program: 62704H
11. CONTROLLING OFFICE NAME AND ADDRESS Director Defense Nuclear Agency Washington, DC 20305		12. REPORT DATE November 1975 13. NUMBER OF PAGES 35
14. MONITORING AGENCY NAME & ADDRESS *(if different from Controlling Office)*		15. SECURITY CLASS. *(of this report)* UNCLASSIFIED 15a. DECLASSIFICATION/DOWNGRADING SCHEDULE

16. DISTRIBUTION STATEMENT *(of this Report)*

Approved for public release; distribution unlimited

17. DISTRIBUTION STATEMENT *(of the abstract entered in Block 20, if different from Report)*

18. SUPPLEMENTARY NOTES

AMCMS Code: 6910002210917 HDL Project No.: E194E2
This work was sponsored by the Defense Nuclear Agency under Subtask R99QAXEBO75 and Work Unit 43/Current Injection Techniques for C^3 Applications.

19. KEY WORDS *(Continue on reverse side if necessary and identify by block number)*

Shielded cables
EMP
Shielding effectiveness
Current injection

20. ABSTRACT *(Continue on reverse side if necessary and identify by block number)*

This note presents a resistive-inductive circuit representation of the coupling of transient currents to partially shielded conductors. The current coupled to the inner conductors is computed in terms of the shield current by use of lumped parameters directly related to the specific geometry of a given problem. The model is applied to an example where experimental

DD FORM 1 JAN 73 1473 EDITION OF 1 NOV 65 IS OBSOLETE

UNCLASSIFIED

SECURITY CLASSIFICATION OF THIS PAGE *(When Data Entered)*

data are available; the peak value of the coupled current is a significant fraction of the exciting current; that is, the shield is effectively short-circuited.

CONTENTS

FIGURES

1. INTRODUCTION

The degree of electrical isolation or shielding between two segments of a conducting structure is frequently determined by measuring induced transient currents in one of the segments when a known current is injected into the other. Typically, a current pulse $i_p(t)$ is generated on a grounded cable shield by a small transient source, and the resulting current on an internal bundle $i_s(t)$ is measured (fig. 1). A low ratio of peak bundle current to shield current generally indicates a high degree of isolation, and conversely, a high ratio of currents indicates poor isolation. If the cable shield were completely continuous and surrounded the entire length of the internal bundle, this ratio would be small indeed, because the current induced on the internal bundle would be solely due to fields directly penetrating the shield, and such fields would have been attenuated by hundreds of decibels in passing through the walls of a typical shield at most frequencies of interest. Unfortunately, most cable shields are not completely continuous and do not surround the internal bundle over its entire length. There are often direct resistive, inductive, and even capacitive coupling routes between the outside of the shield and the internal bundle, which effectively bypass the high-loss path through the shield. It is then found that currents generated on the internal bundle greatly exceed the currents that would have been produced if direct penetration of the shield had been the only coupling route available. In other words, a discontinuous or incomplete cable shield can be partially or wholly short-circuited by direct coupling between shield and bundle.

Figure 2 represents a frequent situation. Here a cable shield, grounded at both ends, surrounds a section of a bundle that also is grounded at both ends through load impedances. If a current $i_p(t)$ is

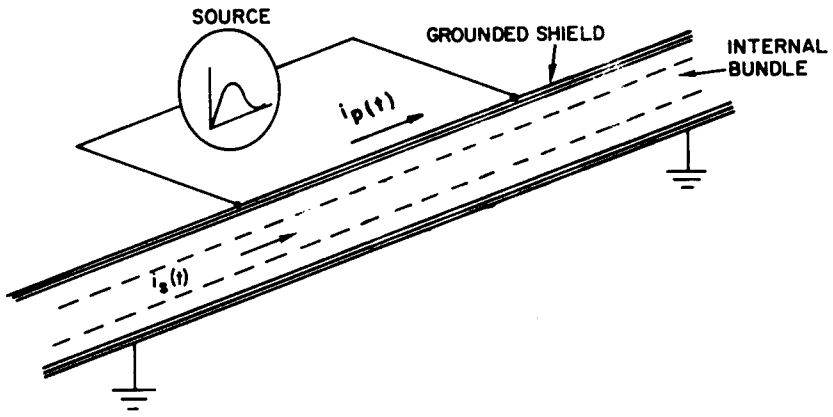

Figure 1. Current source driving a grounded cable shield containing an internal bundle (end effects ignored).

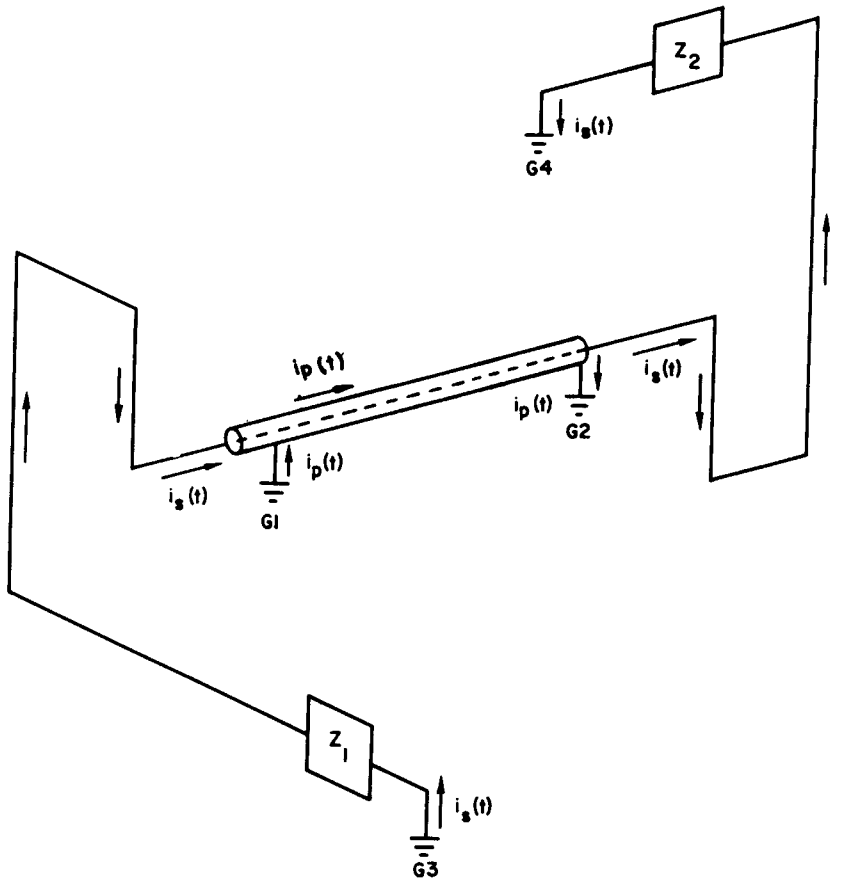

Figure 2. Partially shielded bundle grounded at both ends through load impedances Z_1 and Z_2.

generated on the shield by a small source, $i_p(t)$ can contribute in three ways to the bundle current $i_s(t)$, in addition to directly penetrating the shield wall:

(a) Resistive coupling through the grounding system

(b) Inductive coupling between the outside of the shield and those segments of the bundle conductor that are not surrounded by the shield

(c) Capacitive coupling between the outside of the shield and the exposed segments of the bundle conductor.

Resistive coupling depends on the resistances between the four grounds taken in pairs; inductive coupling depends on the length and orientation of the bundle conductor with respect to the shield; and capacitive coupling depends on the surface areas and distance between

the shield and bundle, among other factors. In such a situation, one should not be surprised if the performance of the cable shield in electrically isolating the internal bundle is rather poor.

This report presents an R,L circuit representation of the situation depicted in figure 2 (capacitive coupling is ignored) that permits one to compute $i_s(t)$ in terms of $i_p(t)$ using lumped parameters directly related to the specific geometry of a given problem. The model is applied to an example where experimental data are available, and it is verified that the peak value of $i_s(t)$ is indeed a significant fraction of $i_p(t)$; that is, the shield is effectively short-circuited.

2. CIRCUIT MODEL

For a circuit model of the partially shielded bundle, the distributed resistances, inductances, and capacitances along and between the shield and the bundle must be replaced by lumped equivalents of near equivalents. For example, the distributed self-inductance of the shield, which in fact is a complicated function of frequency, must be replaced by a constant L_p corresponding to a single impedance element of the form $j2\pi fL_p$, where f is the frequency. This constant must, of course, be an adequate approximation to the actual self-inductance of the shield over the frequency range of interest. Similarly, the distributed self-inductance of the bundle is replaced by a constant L_s; the distributed mutual inductance linking the shield and the bundle is replaced by a constant M; and the ground resistances linking G1, G2, G3, and G4 are replaced by constants R_{12}, R_{13}, R_{14}, R_{23}, R_{24}, and R_{34}.

Generally, a lumped parameter model for a distributed structure is valid when the longest dimension of the structure is significantly smaller than the shortest wavelength of interest in the current pulse. For example, a current pulse with a rise time of 10^{-6} s contains important amounts of energy at frequencies as high as 10^6 Hz. A frequency of 10^6 Hz corresponds to a free space wavelength of 300 m. Hence, with this current source, a lumped parameter model for a partially shielded bundle of conductors would probably be valid for conductor lengths of 100 m or less. This report is limited to sources with significant frequencies below 10 MHz. In this frequency range, distributed capacitances can be expected to be much less important than resistances and inductances in coupling energy from the shield into the bundle. Consequently, distributed capacitances are ignored as a first approximation in the following. However, load capacitances (that is, condensers in Z_1 or Z_2) are not ignored, for these can have an important effect on the bundle current.

The first step in constructing a circuit model is to note that the source loop in figure 2 is small compared to the rest of the structure and is equivalent to a current source $i_p(t)$ ($I_p(f)$ in the frequency domain) on the cable shield. Thus, there are two basic loops to consider. A primary loop consists of a path along the cable shield and through the ground (fig. 3, where R_p is the ground resistance between G1 and G2 in fig. 2 and L_p is the self-inductance of the shield). A secondary loop consists of a path through the load impedances Z_1 and Z_2, the internal bundle and the ground (fig. 4,

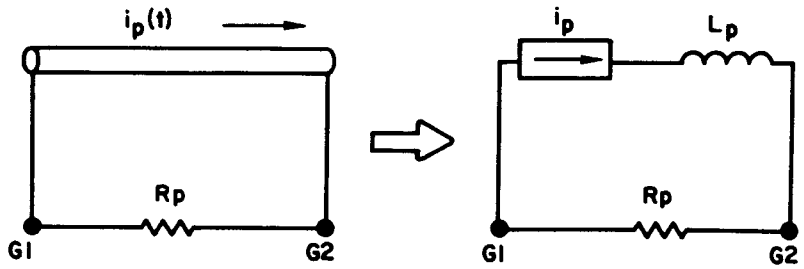

Figure 3. Primary loop.

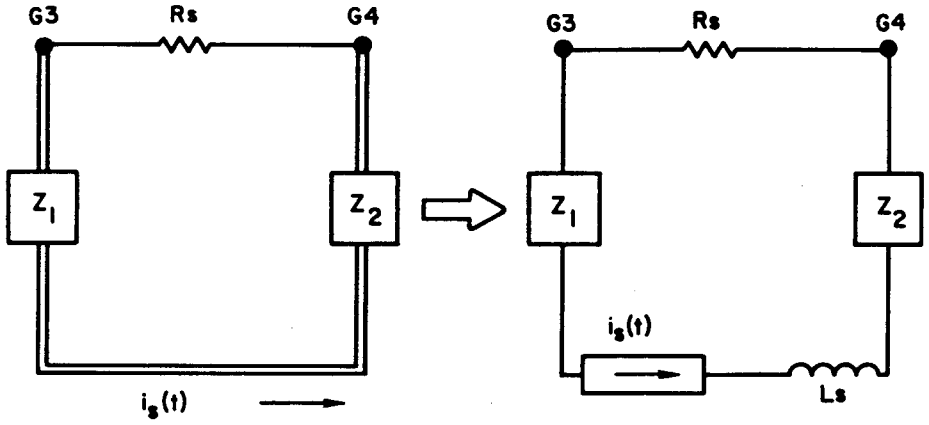

Figure 4. Secondary loop.

where R_S is the ground resistance between G3 and G4, and L_S is the self-inductance of the bundle). These two loops are inductively coupled through the mutual inductance between the shield and the bundle, and they are resistively coupled through ground paths connecting G1 and G3, G1 and G4, G2 and G3, and G2 and G4. Thus, in the circuit model shown in figure 5, M is the mutual inductance between the shield and the bundle, and R_{13}, R_{14}, R_{23}, and R_{24} are the resistances through the ground paths connecting G1 and G3, G1 and G4, etc. Sometimes in practice, the return path in the secondary loop is not through the ground, but directly through the load impedances Z_1 and Z_2. When it is, there is no resistive coupling between the primary and secondary loops, and the only link between the shield and bundle is through the inductive coupling M. This link can be obtained from the model by letting $R_S \to 0$.

The circuit in figure 5 is to be solved in the frequency domain for $I_S(f)$ in terms of $I_p(f)$ and the resulting expression transformed into the time domain $i_s(t)$ by taking the inverse Laplace transform.

Skilling[1] describes a method of solving networks with current sources and inductive coupling using node equations. This method relies on branch equations and connection equations from Kirchhoff's laws. Since there are eight branches and three independent nodes in figure 5, this approach obtains a system of 11 equations in 11 unknowns. Fortunately, this system can be reduced quite easily to an equivalent set of seven equations with seven branch currents as the unknowns:

$$
\begin{aligned}
I_s + I_{34} + I_{13} + I_{23} + 0 + 0 + 0 &= 0 \\
0 + 0 - I_{13} + 0 + I_{14} + I_{12} + 0 &= -I_p \\
0 + 0 + 0 - I_{23} + 0 - I_{12} + I_{24} &= I_p \\
AI_s - R_s I_{34} + 0 + 0 + 0 + 0 + 0 &= -j2\pi fMI_p \\
j2\pi fMI_s + 0 + 0 + 0 + 0 - R_p I_{12} + 0 &= -j2\pi fL_p I_p \\
0 - R_s I_{34} + 0 + R_{23} I_{23} + 0 + 0 + R_{24} I_{24} &= 0 \\
0 - R_s I_{34} + R_{13} I_{13} + 0 + R_{14} I_{14} + 0 + 0 &= 0
\end{aligned}
\qquad (1)
$$

where I_{12} is the current in the branch connecting G1 and G2, I_{14} is the current in the branch connecting G1 and G4, and I_{13}, I_{23}, I_{24}, and I_{34} are defined similarly. All other quantities are as previously defined, except

$$A = Z_1 + Z_2 + j2\pi fL_s \ . \qquad (2)$$

The solution to this system, though tedious, is quite straightforward with determinants. Omitting the details,

$$I_s(f) = \left[\frac{R_s W R_p + j2\pi fMR_p Y + j2\pi fL_p R_s W}{R_s R_p X + j2\pi fMR_s W + AR_p X} \right] I_p(f) \qquad (3)$$

where

$$W = R_{23}R_{14} - R_{13}R_{24} \qquad (4)$$

$$X = (R_{24} + R_{23})(R_{14} + R_{13}) \qquad (5)$$

$$Y = X + R_s(R_{24} + R_{23} + R_{14} + R_{13}) . \qquad (6)$$

---

[1] *H. H. Skilling, Electrical Engineering Circuits, John Wiley & Sons, Inc., New York (1965), 336.*

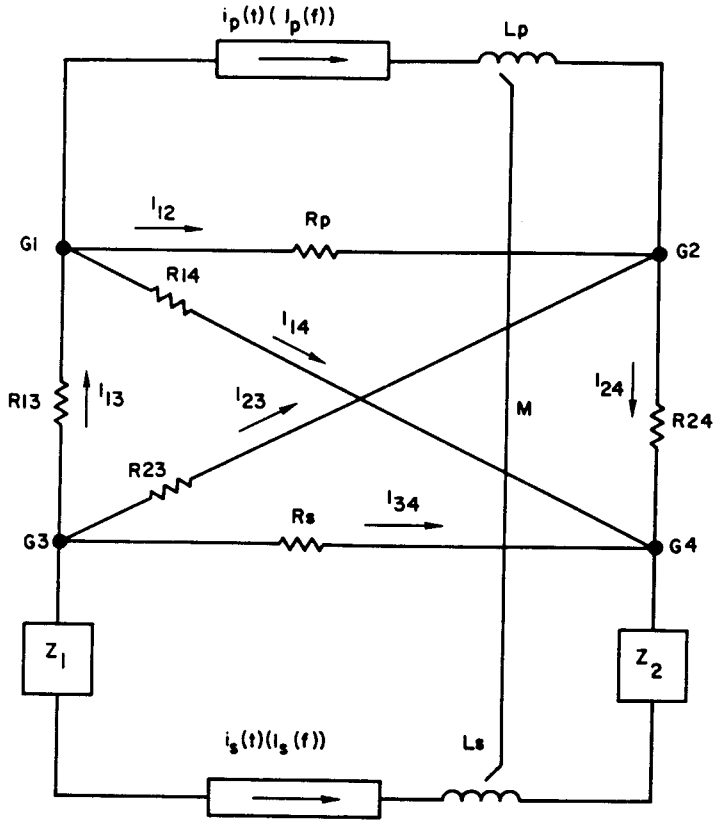

Figure 5. Partially shielded bundle.

Equation (3) is the desired expression relating the shield and bundle currents in the frequency domain. Since equation (3) is derived from a circuit model, it will always be possible to carry out the inverse Laplace transform to obtain an explicit expression for $i_s(t)$, provided $I_p(f)$ is sufficiently well-behaved. This report is limited to shield currents of the form

$$I_p(f) = I\left(\frac{1}{E + j2\pi f} - \frac{1}{F + j2\pi f}\right) \tag{7}$$

where the inverse transformation of equation (3) is straightforward. The time domain representation of equation (7) is the difference between two decaying exponentials:

$$i_p(t) = I\left(e^{-Et} - e^{-Ft}\right). \tag{8}$$

Since most current pulses of interest can be approximated by linear combinations of terms like equation (8), limitation of $I_p(f)$ to the form given by equation (7) does not seriously restrict the theory.

3. LUMPED PARAMETERS

The accuracy of any model is no better than the accuracy of the parameters that go into it. Thus, if the present model is to have any chance of success, the ground resistances and self- and mutual inductances must be determined with sufficient accuracy to at least preserve in a general way the correct relationships among circuit elements. One might prefer to measure these quantities directly, but could do so only rarely with existing structures, since direct measurement would require that the structure be at least partially dismantled. Then usually one must attempt to estimate these quantities from the best available information. Ground resistances can frequently be estimated from measurements at the time of construction, since grounding systems must usually be certified to meet specifications. If this information is not available, standard formulas such as those given by Sunde[2] can be used to compute ground resistances, provided the grounding elements correspond reasonably well to those few types for which formulas have been developed, and provided the soil conductivity is known. For inductances, one is limited to estimates based on calculations, since these quantities are not usually certified at the time of construction. The formulas compiled by Grover[3] are very useful in such estimating.

Figure 6 illustrates the use of inductance formulas. The heavy solid line represents an exposed conductor connecting the ground G and the cable shield, which is shown as three parallel dashed lines. The lighter solid line is an exposed segment of the internal bundle starting at the point T where the shield terminates. The coefficient of mutual inductance M between the ground line and the exposed internal bundle is to be computed. In practice, one would compute also the mutual inductance between the cable shield and the internal bundle. However, since the same method can be used in both calculations, the latter is ignored here. Each conductor consists of a series of straight segments, and the lengths of these segments are much greater than the diameters. Each segment may be considered a straight line current filament of zero diameter. The mutual inductance between ground line and bundle can be computed by first calculating the mutual inductances between all pairs of segments consisting of one filament from the ground line and one from the bundle and then adding these contributions to obtain the total. These pair-wise calculations use a general formula giving the mutual inductance between two straight filaments placed in any desired position.[3] Figure 7 shows two such filaments of lengths ℓ and m in arbitrary positions with respect to a rectangular coordinate system.

---

[2] *E. D. Sunde, Earth Conduction Effects in Transmission Systems, D. Van Nostrand Co., Inc., Princeton (1943).*

[3] *F. W. Grover, Inductance Calculations: Working Formulas and Tables, Dover Publications, Inc., New York (1962).*

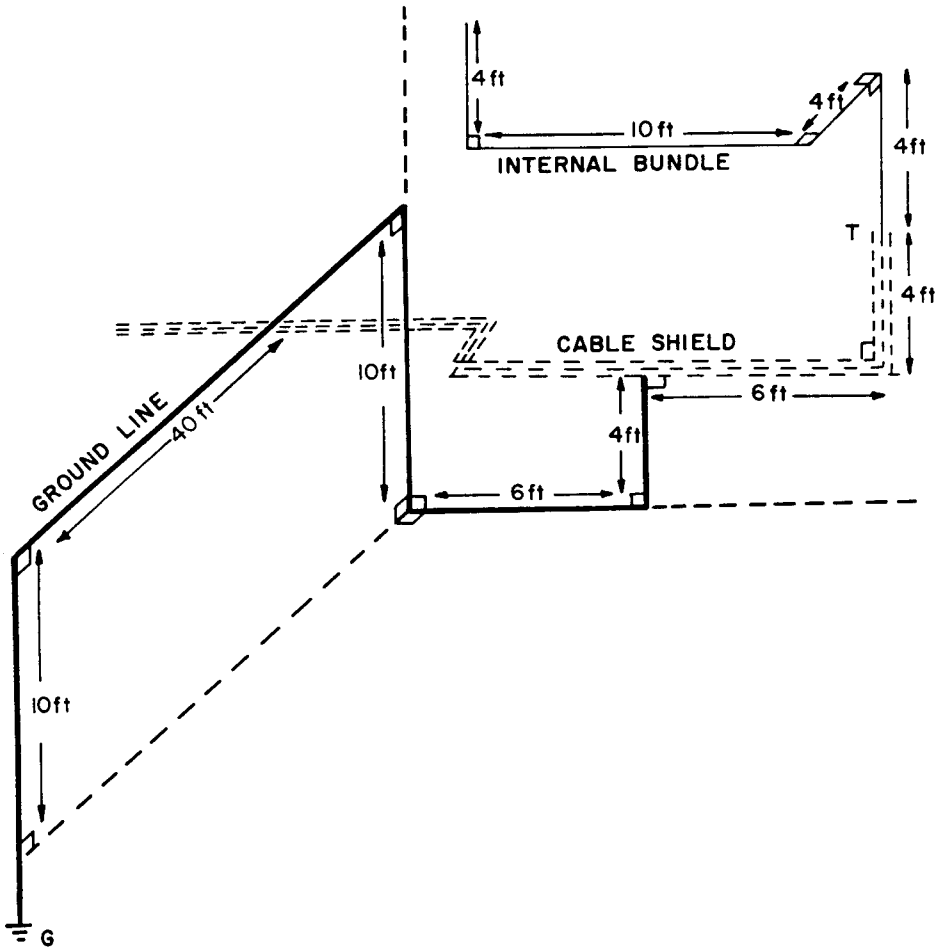

Figure 6. Ground conductor (heavy line) and partially exposed bundle (light line).

If the coordinates of the end points of the first filament are (x_1, y_1, z_1) and (x_2, y_2, z_2) and the coordinates of the end points of the second are (x_1', y_1', z_1') and (x_2', y_2', z_2'), then ℓ and m are given by

$$\ell = \left((x_1 - x_2)^2 + (y_1 - y_2)^2 + (z_1 - z_2)^2 \right)^{\frac{1}{2}}$$
$$m = \left((x_1' - x_2')^2 + (y_1' - y_2')^2 + (z_1' - z_2')^2 \right)^{\frac{1}{2}} \qquad (9)$$

and the distances D_1, D_2, D_3, and D_4 are

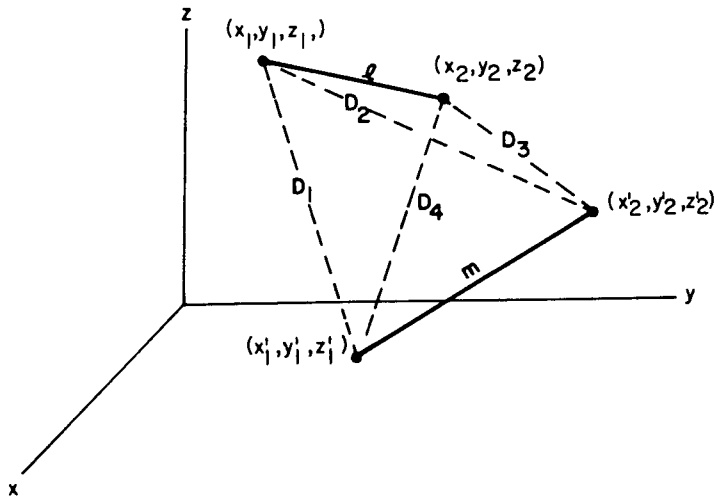

Figure 7. Two arbitrarily positioned filaments of lengths ℓ and m.

$$
\begin{aligned}
D_1 &= \left((x_1 - x_1')^2 + (y_1 - y_1')^2 + (z_1 - z_1')^2\right)^{\frac{1}{2}} \\
D_2 &= \left((x_1 - x_2')^2 + (y_1 - y_2')^2 + (z_1 - z_2')^2\right)^{\frac{1}{2}} \\
D_3 &= \left((x_2 - x_2')^2 + (y_2 - y_2')^2 + (z_2 - z_2')^2\right)^{\frac{1}{2}} \\
D_4 &= \left((x_2 - x_1')^2 + (y_2 - y_1')^2 + (z_2 - z_1')^2\right)^{\frac{1}{2}}
\end{aligned}
\tag{10}
$$

The mutual inductance M between the two filaments is given by

$$
\begin{aligned}
\frac{M}{0.002 \cos \varepsilon} &= (\mu + \ell) \tanh^{-1} \frac{m}{D_1 + D_2} \\
&\quad + (\nu + m) \tanh^{-1} \frac{\ell}{D_1 + D_2} \\
&\quad - \mu \tanh^{-1} \frac{m}{D_3 + D_4} \\
&\quad - \nu \tanh^{-1} \frac{\ell}{D_2 + D_3} - \frac{\Omega d}{2 \sin \varepsilon}
\end{aligned}
\tag{11}
$$

where

$$\Omega = \tan^{-1}\left(\frac{d^2 \cos\varepsilon + (\mu+\ell)(\nu+m)\sin^2\varepsilon}{dD_1 \sin\varepsilon}\right) - \tan^{-1}\left(\frac{d^2 \cos\varepsilon + (\mu+\ell)\nu\sin^2\varepsilon}{dD_2 \sin\varepsilon}\right) + \tan^{-1}\left(\frac{d^2 \cos\varepsilon + \mu\nu\sin^2\varepsilon}{dD_3 \sin\varepsilon}\right) - \tan^{-1}\left(\frac{d^2 \cos\varepsilon + \mu(\nu+m)\sin^2\varepsilon}{dD_4 \sin\varepsilon}\right) \tag{12}$$

and

$$\cos\varepsilon = \alpha^2/2\ell m \tag{13}$$

$$\alpha^2 = D_4^2 - D_3^2 + D_2^2 - D_1^2 \tag{14}$$

$$d^2 = D_3^2 - \mu^2 - \nu^2 + 2\mu\nu\cos\varepsilon \tag{15}$$

$$\mu/\ell = \frac{2m^2\left(D_2^2 - D_3^2 - \ell^2\right) + \alpha^2\left(D_4^2 - D_3^2 - m^2\right)}{4\ell^2m^2 - \alpha^4} \tag{16}$$

$$\nu/m = \frac{2\ell^2\left(D_4^2 - D_3^2 - m^2\right) + \alpha^2\left(D_2^2 - D_3^2 - \ell^2\right)}{4\ell^2m^2 - \alpha^4} . \tag{17}$$

In these formulas, all distances are in centimeters, and the mutual inductance is given in microhenrys. On the basis of equations (9) to (17), it is a straightforward matter to write a computer program that will take the coordinates of the end points and compute the mutual inductance between any pair of current filaments. To facilitate the use of such a program, it is convenient to introduce a coordinate system into figure 6 and to specify the coordinates at each end of every segment. With the aid of figure 8, one can compute the mutual inductance between ground line and bundle by applying this program to all pairs of segments comprising the ground line and bundle and adding up the results. Since the ground line has five segments and the bundle has four, there are 20 distinct pairs, each of which is composed of one segment from the ground line and one from the bundle.

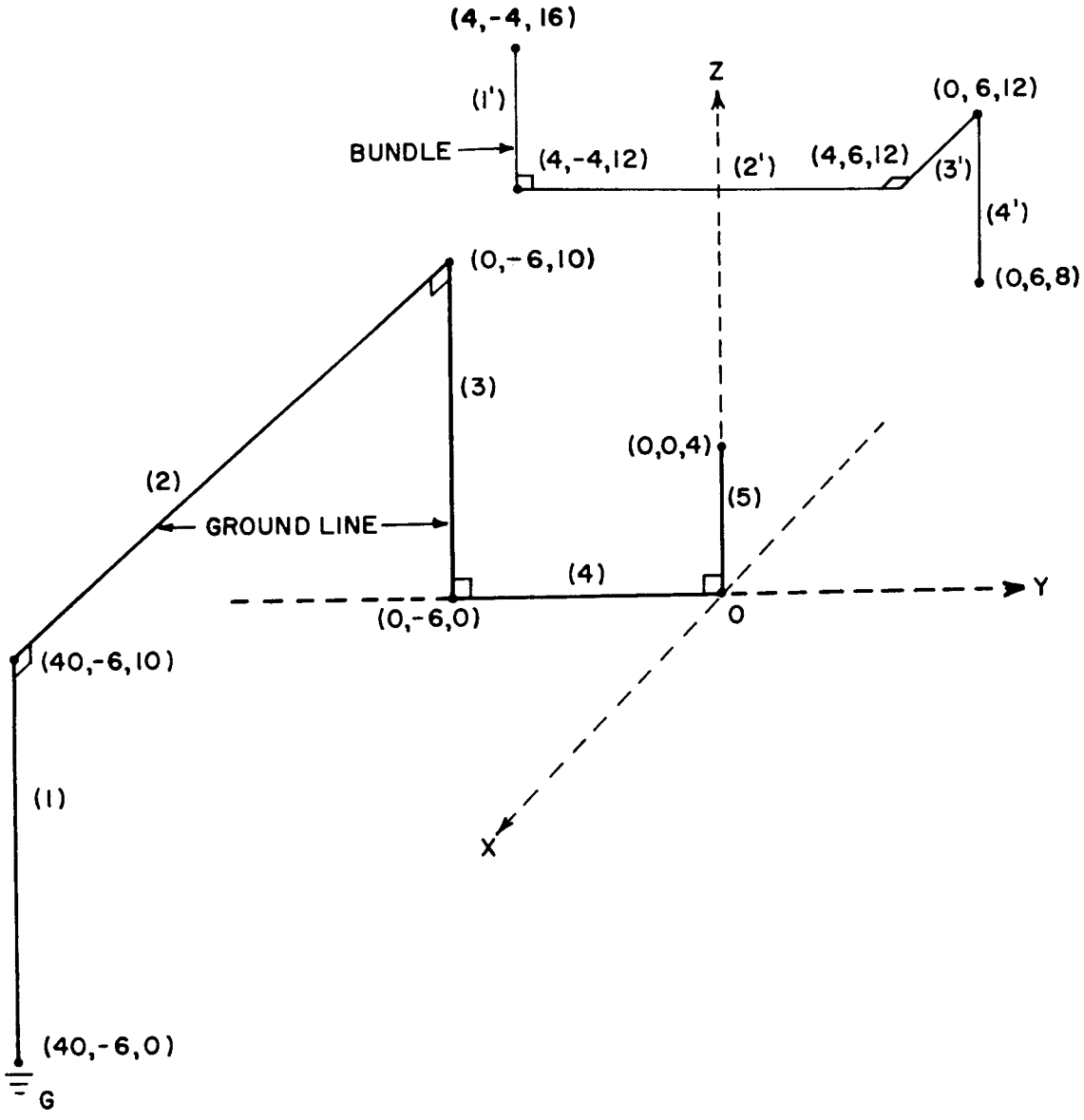

Figure 8. Reconstruction of figure 6 with the coordinates of each segment specified in a rectangular system.

Designating M(1,1') as the mutual inductance between segments labeled 1 and 1' in figure 8, M(1,2') as the mutual inductance between segments 1 and 2', and so on, one obtains the following:

$M(1,1') = 0.0327\ \mu H$ $\quad$ $M(2,1') = 0$

$M(1,2') = 0$ $\quad$ $M(2,2') = 0$

$M(1,3') = 0$ $\quad$ $M(2,3') = 0.341\ \mu H$

$M(1,4') = 0.0289\ \mu H$ $\quad$ $M(2,4') = 0$

$M(3,1') = 0.189\ \mu H$ $\quad$ $M(4,1') = 0$

$M(3,2') = 0$ $\quad$ $M(4,2') = 0.136\ \mu H$

$M(3,3') = 0$ $\quad$ $M(4,3') = 0$

$M(3,4') = 0.0909\ \mu H$ $\quad$ $M(4,4') = 0$

$M(5,1') = 0.0329\ \mu H$

$M(5,2') = 0$

$M(5,3') = 0$

$M(5,4') = 0.0635\ \mu H$

The mutual inductance between perpendicular segments is 0, as expected. The total mutual inductance is then the sum of the preceding 20 quantities:

$$M = M(1,1') + M(1,2') + \ldots + M(5,4')$$

$$= 0.0327 + 0.0289 + 0.341 + 0.189 + 0.0909 + 0.136 + 0.0329 + 0.0635\ \mu H$$

$$= 0.915\ \mu H.$$

The self-inductance of a circuit composed of straight segments equals the sum of the mutual inductances of all pairs of filaments of which it is composed, plus the sum of the self-inductances of all segments of which it is composed. Therefore, the preceding formulas can be used also with the general expression for the self-inductance L of straight round wire of radius ρ and length λ:

$$L = 0.002\lambda \left[\ln\left(\frac{2\lambda}{\rho}\right) - \frac{3}{4}\right] \qquad (18)$$

to compute L_s and L_p for use in equation (3).[3]

[3] *F. W. Grover, Inductance Calculations: Working Formulas and Tables, Dover Publications, Inc., New York (1962).*

4. TRANSIENT BUNDLE CURRENTS

This section applies the inverse Laplace transform to equation (3) with $I_p(f)$ given by equation (7) and obtains explicit time domain expressions for the bundle current $i_s(t)$. For these calculations, the load impedance $Z_s = Z_1 + Z_2$ must be specified. Two cases are considered, depending on the values assigned to Z_s. In the first case, Z_s is a pure resistance R, and in the second, it is a pure reactance equal to that of a single condenser (capacitive load). As one would expect, $i_s(t)$ is quite different in these two cases.

4.1 Case 1, $Z_s = R$

With a resistive load, equation (3) can be written

$$I_s(f) = I \left[\frac{A + j2\pi fB}{C + j2\pi fD}\right] \left[\frac{1}{E + j2\pi f} - \frac{1}{F + j2\pi f}\right]$$

where

$$A = R_s W R_p \tag{20}$$

$$B = MR_pY + L_pR_sW \tag{21}$$

$$C = R_pX\left(R_s + R\right) \tag{22}$$

$$D = MR_sW + L_sR_pX. \tag{23}$$

Equation (19) can be cast into another form suitable for easy transformation by use of partial fraction expansions of the type

$$\frac{1}{\alpha + j2\pi f\beta} \cdot \frac{1}{\gamma + j2\pi f} = \frac{\xi}{\alpha + j2\pi f\beta} + \frac{\zeta}{\gamma + j2\pi f}$$

where

$$\zeta = \frac{1}{\alpha - \beta\gamma}$$

$$\xi = -\beta\zeta .$$

Omitting the details,

$$i_s(t) = I\left[\frac{(F - E)\ (AD - BC)}{(C - DE)\ (C - DF)}\ e^{-\frac{Ct}{D}}\right.$$

$$\left. + \frac{(A - BE)}{(C - DE)}\ e^{-Et} - \frac{(A - BF)}{(C - DF)}\ e^{-Ft}\right]. \tag{24}$$

Figure 9 plots $i_p(t)$ and $i_s(t)$ computed from equations (8) and (24), respectively, by use of several values of M as indicated and the following values for remaining parameters:

$L_s = 20\ \mu H$ $\qquad$ $L_p = 20\ \mu H$

$R_s = 40\ \Omega$ $\qquad$ $R_p = 50\ \Omega$

$R_{13} = 20\ \Omega$ $\qquad$ $R_{24} = 20\ \Omega$

$R_{14} = 40\ \Omega$ $\qquad$ $R_{23} = 40\ \Omega$

$R = 0$

$E = 5 \times 10^5\ s^{-1}$ $\qquad$ $F = 4 \times 10^7\ s^{-1}$

In figure 9, the amplitude factor I is chosen to produce a peak value for $i_p(t)$ of 1 A. Thus, from equation (8), I is given explicitly as follows:

$$I = \frac{1}{e^{-Et_{max}} - e^{-Ft_{max}}} \tag{25}$$

where t_{max} is the time at which $i_p(t)$ attains its maximum value. From equation (8), it can be shown that

$$t_{max} = \frac{\ln\left(\frac{E}{F}\right)}{E - F}\ . \tag{26}$$

For E and F as given above, t_{max} = 111 ns = 111 x 10-9 s.

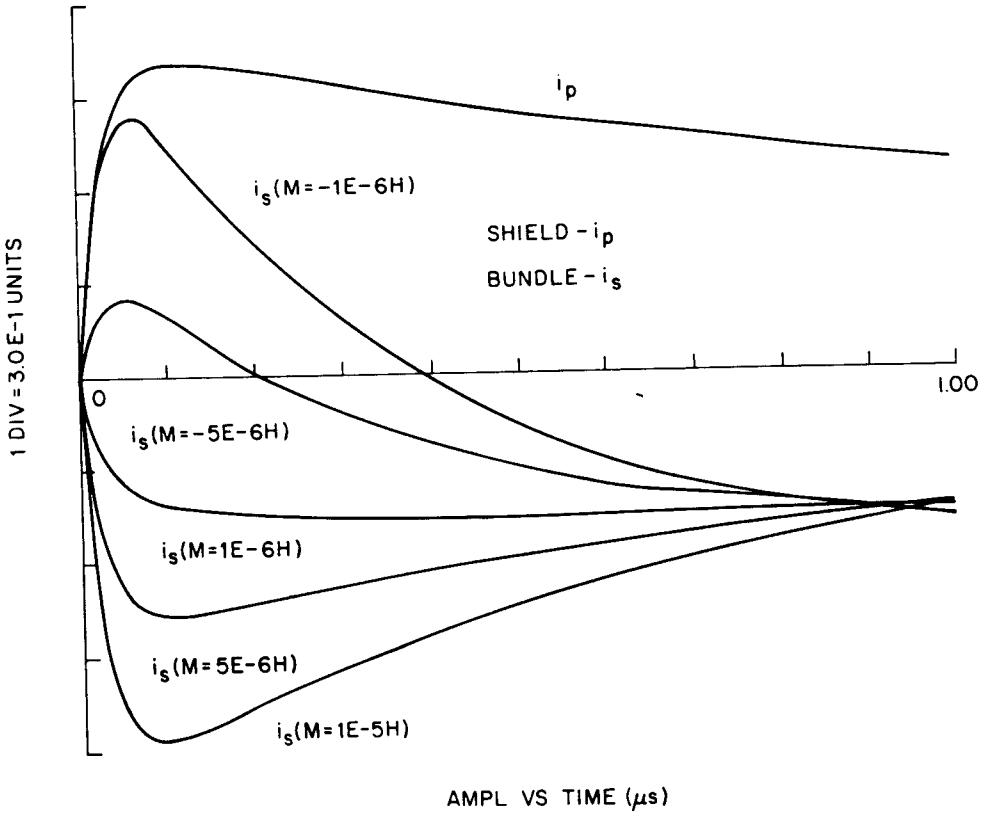

Figure 9. Theoretical shield and bundle currents for the case of a resistively loaded bundle.

Figure 9 indicates that in this case, bundle current is quite similar to shield current in shape and in peak value. As M increases through positive values, the peak current increases in magnitude, and the rise time decreases. That i_S is opposite in sign to i_p when M is positive means that i_S is flowing in the opposite direction to that assumed in figure 5. When M is negative, both the peak values and the rise time increase as M assumes larger negative values.

4.2 Case 2, Capacitive Load

When the load in the secondary circuit consists of a condenser with capacitance C_S, then

$$Z_s = \frac{1}{j2\pi f C_s} \tag{27}$$

and equation (3) becomes

$$I_s(f) = I\left[\frac{R_sWR_p + j2\pi fMR_pY + j2\pi fL_pR_sW}{R_sR_pX + j2\pi fMR_sW + \left(\frac{1}{j2\pi fC_s} + j2\pi fL_s\right)R_pX}\right]$$

$$\cdot\left[\frac{1}{E + j2\pi f} - \frac{1}{F + j2\pi f}\right]$$

which can be rewritten

$$I_s(f) = \frac{Ij2\pi f}{D}\left[\frac{P + Qj2\pi f}{U + Vj2\pi f + (j2\pi f)^2}\right] \cdot\left[\frac{1}{E + j2\pi f} - \frac{1}{F + j2\pi f}\right] \tag{28}$$

where

$$P = R_sWR_p \tag{29}$$

$$Q = MR_pY + L_pR_sW \tag{30}$$

$$D = MR_sW + L_sR_pX \tag{31}$$

$$U = R_pX/C_sD \tag{32}$$

$$V = R_sR_pX/D\ . \tag{33}$$

With the aid of a partial fraction expansion, equation (28) becomes

$$I_s(f) = \left(\frac{I}{D}\right) j2\pi f(P + Qj2\pi f) \left(\frac{Qj2\pi f + \psi}{U + Vj2\pi f + (j2\pi f)^2}\right. \tag{34}$$

$$\left. + \frac{\gamma}{E + j2\pi f} - \frac{\gamma'}{F + j2\pi f}\right)$$

where

$$\gamma = \frac{1}{E(E - V) + U} \tag{35}$$

$$\gamma' = \frac{1}{F(F - V) + U} \tag{36}$$

$$\psi = (E - V)\gamma - (F - V)\gamma' \ . \tag{37}$$

When the factors in the numerator are multiplied, equation (34) becomes

$$I_s(f) = \left(\frac{I}{D}\right)\left[\left(Q\phi(j2\pi f)^3 + (Q\psi + P\phi)(j2\pi f)^2\right.\right.$$

$$\left. + P\psi(j2\pi f)\right)\left(\frac{1}{U + V(j2\pi f) + (j2\pi f)^2}\right) \tag{38}$$

$$\left. + \left(P(j2\pi f) + Q(j2\pi f)^2\right)\left(\frac{\gamma}{E + j2\pi f} - \frac{\gamma'}{F + j2\pi f}\right)\right]$$

where

$$\phi = \gamma' - \gamma \ . \tag{39}$$

Now the inverse Laplace transform of equation (38) can be written by inspection with the aid of the following pairs:[4]

$$\mathcal{L}^{-1}\left[\frac{1}{U + Vj2\pi f + (j2\pi f)^2}\right] = \frac{e^{-\frac{Vt}{2}} \sin \omega t}{\omega} \tag{40}$$

where

$$\omega = \left(U - \frac{V^2}{4}\right)^{\frac{1}{2}} \quad \text{and } U > \frac{V^2}{4} \text{ is assumed,} \tag{41}$$

$$\mathcal{L}^{-1}\left[\frac{1}{a + j2\pi f}\right] = e^{-at} \tag{42}$$

$$\mathcal{L}^{-1}\left[(j2\pi f)^n F(j2\pi f)\right] = \frac{d^n f(t)}{dt^n} \tag{43}$$

where

$$f(t) = \mathcal{L}^{-1}\left[F(j2\pi f)\right].$$

Thus, the time domain representation of the secondary current is

$$i_s(t) = \frac{I}{D}\left[\left(Q\phi\frac{d^3\cdot}{dt^3} + (Q\psi + P\phi)\frac{d^2\cdot}{dt^2} + P\psi\frac{d\cdot}{dt}\right)\frac{e^{-\frac{Vt}{2}} \sin \omega t}{\omega} + \left(P\frac{d\cdot}{dt} + Q\frac{d^2\cdot}{dt^2}\right)\left(\gamma e^{-Et} - \gamma' e^{-Ft}\right)\right]. \tag{44}$$

[4] *G. Doetsch, Guide to the Applications of Laplace Transforms, D. Van Nostrand Co., Ltd, London (1961).*

After the differentiations and the collection of like terms are carried out,

$$i_s(t) = \frac{I}{D}\left[\frac{e^{-\frac{Vt}{2}}}{\omega}(\sigma \sin \omega t + \rho \cos \omega t) + \tau e^{-Et} + \mu e^{-Ft}\right] \quad (45)$$

where

$$\sigma = Q\phi V\left(\frac{3\omega^2}{2} - \frac{V^2}{8}\right) + (Q\psi + P\phi)\left(\frac{V^2}{4} - \omega^2\right) - \frac{P\psi V}{2} \quad (46)$$

$$\rho = Q\phi\omega\left(\frac{3V^2}{4} - \omega^2\right) - V\omega(Q\psi + P\phi) + P\psi\omega \quad (47)$$

$$\tau = \gamma E(-P + QE) \quad (48)$$

$$\mu = \gamma' F(P - QF) \quad (49)$$

and the remaining quantities are as defined previously. Figure 10 plots equation (45) (bottom curve) along with equation (8) (top curve) for the following parameters:

$L_p = 20\ \mu H$ $\quad L_s = 20\ \mu H$ $\quad M = 2\ \mu H$

$R_s = 10\ \Omega$ $\quad R_p = 10\ \Omega$

$R_{13} = 5\ \Omega$ $\quad R_{24} = 5\ \Omega$

$R_{14} = 10\ \Omega$ $\quad R_{23} = 10\ \Omega$

$C = 10^{-7}\ F = 0.1\ \mu F$

$E = 2.5 \times 10^5\ s^{-1}$ $\quad F = 2.5 \times 10^7\ s^{-1}$

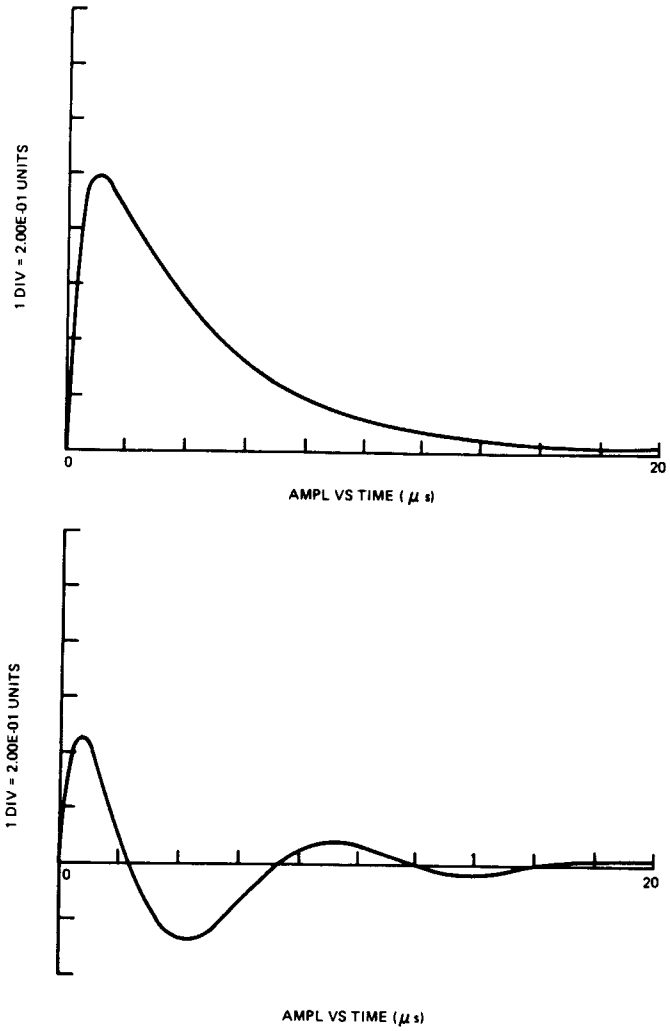

Figure 10. Theoretical shield (top) and bundle (bottom) currents for the case of a capacitively loaded bundle.

Figure 10 shows the type of oscillatory behavior that one might have expected in an R,L circuit with a capacitive load. Although differing in this respect from the curves in figure 9, these curves are similar to the latter in two other respects: The rise time of the secondary current is approximately the same as that of the primary, and the peak secondary current is a significant fraction of the peak primary current.

5. DISCUSSION

The preceding sections have described a circuit model for a partially shielded bundle of conductors. Calculations based on representative (assumed) sets of lumped parameters have indicated that

this model will predict rise times and peak currents on the bundle of the same order of magnitude as those on the shield. Experimental data and theoretical curves obtained by use of computed (or measured) input parameters are not compared here in detail. But one set of measured curves at least qualitatively supports the model. Figure 11 is the shield current, and figure 12 is the corresponding bundle current measured on partially shielded conductors forming a section of a large radio transmitter. The curves have been normalized to a peak shield current of 1 A, and the scale of figure 12 has been expanded. Rise times range from 250 to 500 ns, and the peak bundle current equals approximately 13 percent of the peak shield current. The corresponding values for the computed curves in figure 10 are 700 to 1000 ns and 46 percent, respectively. Considering the uncertainties in the circuit parameters, these represent rather good agreement. Many more such comparisons will be required to determine if these agreements are significant or merely fortuitous.

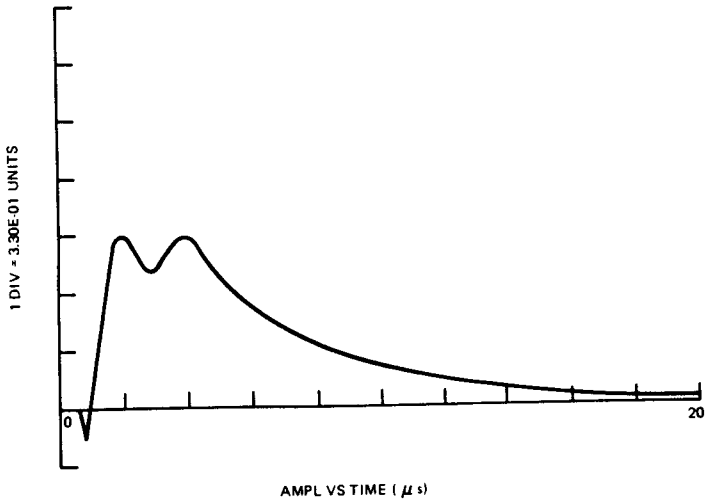

Figure 11. Experimental shield current generated at a radio transmitting facility.

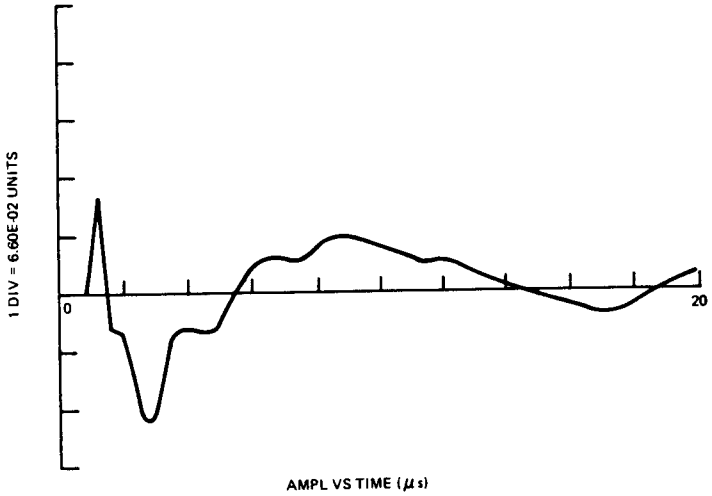

Figure 12. Experimental bundle current caused by the shield current in figure 11.